NMR Studies of Single-File Diffusion in Unidimensional Channel Zeolites

Volker Kukla, Jan Kornatowski, Dirk Demuth, Irina Girnus, Harry Pfeifer, Lovat V. C. Rees, Stefan Schunk, Klaus K. Unger, Jörg Kärger*

Single-file diffusion is the restricted propagation of particles that cannot pass each other. The occurrence of this phenomenon should be reflected by a change in the time dependence of the mean particle displacement in comparison with ordinary diffusion. Although this process is considered to be the rate-controlling mechanism in a large variety of processes, so far no direct evidence of this phenomenon has been provided. Diffusion measurements made with pulsed field gradient nuclear magnetic resonance (NMR) in unidimensional pore systems (zeolites $AlPO_4$-5 and Theta-1) reflect the expected time dependence of single-file diffusion.

Particle propagation in ordered systems of two and more dimensions proceeds by ordinary diffusion. It is reflected by the proportionality between the observation time and the mean square displacement of a tagged particle. As soon as particle movement is restricted to one dimension, substantial deviations may occur. Situations of this type occur in unidimensional (1D) channel systems, which may be found in a large variety of substances and materials. If the channel radii are of the order of the diameters of the moving particles, the individual particles are unable to pass each other as a consequence of their hard-core interaction, and the situation may be compared with a file of strung pearls (*1*). This effect dramatically reduces the translational mobility of any individual particle, and it may be shown theoretically that the mean square displacement will increase only in proportion to the square root of the observation time (*2*). Transport under such conditions has been termed single-file diffusion (*3*).

One of the most important processes in which single-file diffusion plays a crucial role is the transport of ions through biological membranes. In biological systems, the flux ratio often deviates from the ideal value expected for ionic solutions on the basis of the classical Nernst-Planck theory. A quantitative analysis of the influx or efflux of a species of ions through a particular area of the cell membrane (*4*) strongly suggests that the ions are unable to pass each other on their way through the channels within the membranes (*5*). Other examples of single-file diffusion are expected with diffusion in porous materials, including extremely narrow capillaries, synthetic membranes, and microporous solids. The unexpectedly large activation energies that are observed for catalytic reactions in zeolites with a 1D channel structure (*6*), which are in contrast to the small activation energies generally found for transport inhibition in multidimensional pore networks, are thought to be an immediate consequence of intracrystalline single-file diffusion.

In all of these cases, however, the occurrence of single-file diffusion has been postulated only as a mechanism that would provide an excellent microdynamic explanation of the observed dependencies. As far as we know, direct measurements of the proportionality between the mean square displacement of particle propagation and the square root of the observation time have not been reported. We present here a systematic experimental study of this phenomenon in which we apply the pulsed field gradient (PFG) NMR method (*7*, *8*) to zeolites with a 1D channel structure (*9*). We have concentrated in particular on the zeolite $AlPO_4$-5, which has proved to be suitable for the investigation of dimension-dependent processes (*10*). Because synthetic zeolites are available only as crystallites with maximum diameters of 10 to 100 μm, the possibilities of single-crystal structure analysis are rather limited. To circumvent the risk of ambiguity due to structural peculiarities of the given sample, we have carried out studies with zeolite specimens stemming from quite different syntheses.

The usefulness of PFG NMR for tracing single-file diffusion in zeolites has been unclear (*11*). However, progress has been made in both the instrumentation (*12*, *13*) and the data-processing (*14*) of PFG NMR, and these PFG NMR diffusion studies of methane (CH_4) in $AlPO_4$-5 give clear evidence for the proportionality between the mean square displacement and the square root of the observation time. In these measurements, we applied the home-built PFG NMR spectrometer FEGRIS 400 (*12*, *13*), operating at a proton resonance frequency of 400 MHz with field gradient amplitudes up to 24 T m^{-1}. As a typical example of the primary experimental data of the PFG NMR experiment, Fig. 1 presents the intensity Ψ of the NMR signal (the "spin echo") as a function of the quantity $(\gamma\delta g)^2$, where γ denotes the magnetogyric ratio and δ and g stand for the width and amplitude of the field gradient pulses, respectively. We compared the observed signal with that stemming from the gas phase above the bed of zeolite crystallites. We found that the first steep decay is caused by the CH_4 molecules in the gas phase between the individual crystallites. Subtracting this contribution leads to the filled symbols in Fig. 1. The solid line indicates the best fit of the function

$$\Psi = 1/2 \int_{-1}^{1} \exp\left[-\gamma^2\delta^2 g^2 \langle x^2(t)\rangle x^2/2\right] dx \quad (1)$$

to the data points.

Equation 1 represents the theoretical expression for the PFG NMR spin echo attenuation for 1D diffusion along statistically distributed directions (*15*) with a mean square displacement equal to $\langle x^2(t)\rangle$. It is derived from the standard Stejskal-Tanner expression (*16*) with the quantity x introduced as the cosine between the channels and the field gradient direction. The quan-

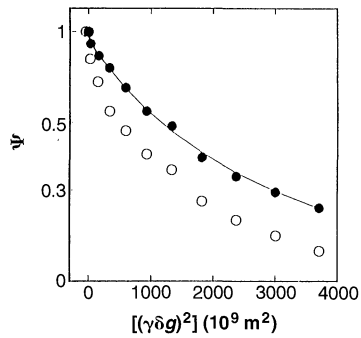

Fig. 1. PFG NMR spin echo attenuation for CH_4 in $AlPO_4$-5 at 293 K for a sorbate concentration of 0.2 molecule per unit cell and an observation time t of 12 ms (open symbols). The filled symbols represent the intensity of the signal stemming from the intracrystalline space as estimated by comparison with the gas-phase signal. The solid line indicates the best fit of Eq. 1 to the data points.

V. Kukla, H. Pfeifer, J. Kärger, Universität Leipzig, Fakultät für Physik und Geowissenschaften, Linnéstraße 5, D-04103 Leipzig, Germany.
J. Kornatowski, RWTH (Technical University), Institut für Technische Chemie und Heterogene Katalyse, Worringerweg 1, D-52074 Aachen, Germany, and Faculty of Chemistry, N. Copernicus University, Gagarina 7, 87-100 Torun, Poland.
D. Demuth, S. Schunk, K. K. Unger, Johannes Gutenberg Universität Mainz, Institut für Anorganische Chemie und Analytische Chemie, J.-J.-Becherweg 24, D-55029 Mainz, Germany.
I. Girnus, Institut für Angewandte Chemie, Rudower Chaussee 5, D-12489 Berlin, Germany.
L. V. C. Rees, Department of Chemistry, University of Edinburgh, West Mains Road, Edinburgh EH9 3JJ, UK.
*To whom correspondence should be addressed.

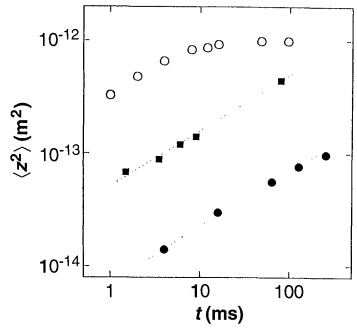

Fig. 2. Molecular mean square displacements resulting from PFG NMR self-diffusion studies at 293 K with CH_4 (○, 0.2 molecule per unit cell) and CF_4 (●, 0.4 molecule per unit cell) in $AlPO_4$-5 and with CH_4 in theta-1 (■, 0.5 molecule per unit cell) as a function of the observation time. The broken lines indicate the dependence $\langle z^2(t) \rangle \propto t^{1/2}$.

tity t is the observation time, which is given by the time span between the field gradient pulses (and which in the terminology of PFG NMR is generally denoted Δ). Here, the direction of molecular displacement is given by that of the channel system. The open symbols in Fig. 2 represent the mean square displacement in the channel direction as a function of the observation time, determined from the best fit of Eq. 1 to the spin echo attenuation. It follows from this representation that the observed time dependence in no way complies with that of ordinary diffusion. For sufficiently small displacements, the mean square displacement is found to increase in proportion to $t^{1/2}$ as required for single-file systems. From this part of the representation, one determines a value of $F = 6 \times 10^{-11}$ m^2 s$^{-1/2}$ for the mobility factor of single-file diffusion, where F is defined by the relation (*11*)

$$\langle z^2(t) \rangle = 2Ft^{1/2} \qquad (2)$$

by analogy to the Einstein equation for normal diffusion. In the case of activated jumps, F has been predicted theoretically (*2*) to be proportional to $(1 - \theta)/\theta$, with θ denoting the relative occupancy.

With increasing observation time, the displacements tend to increase less and less. This effect may be attributable to the influence of transport resistances in the channels, which become significant for displacements ≥3 μm. This value may be considered as a measure of the mean distance between blockages within the channels. This type of information cannot be obtained from the structure analysis by x-ray diffraction, which is insensitive to lattice defects at such a low concentration. The results are thus complementary to the results of studies of the accessibility of the zeolite channel network by polarization microscopy (*17*).

The single-particle diffusivity at infinite dilution corresponding to this mobility factor may be estimated on the basis of simple random-walk considerations (*11*). Within the model applied, the coefficient of single-particle diffusion may attain the order of 10^{-4} m^2 s^{-1}. This value is astonishingly high and exceeds the largest intracrystalline diffusivities observed so far in zeolites (*8*) by four orders of magnitude. A possible explanation for this mobility enhancement may be related to the fact that earlier PFG NMR diffusion studies have generally been carried out with zeolites containing pore networks where the dissipation of momentum for a particular, isolated molecule might be expected to occur much faster than in straight 1D channels. In view of the estimates given in (*11*), the high mobility is indispensable for the PFG NMR measurement of molecular displacements in single-file systems.

The observed time dependence of the mean square displacement of CH_4 in $AlPO_4$-5 is at variance with recent PFG NMR measurements of the same system (*18*) that have yielded 1D normal diffusion. In those studies, however, a much smaller range of observation times was considered (t = 1, 4, 5, and 6 ms), where, in addition, the reliability of the attenuation data for t = 1 ms is probably limited as a result of experimental problems inherent in PFG NMR measurements for short observation times (*7*, *13*). From a mere comparison of the diameters of the molecules [0.38 nm (*19*)] and the channels [0.73 nm (*9*)], it clearly cannot be excluded that the $AlPO_4$-5 structure does permit a mutual passage of the CH_4 molecules within the channels. In this case, the observed $t^{1/2}$ dependence could as well result if the chosen observation times were within the transition range between unrestricted normal diffusion and restricted diffusion.

In order to exclude such a possibility, we have investigated a variety of adsorbate-adsorbent systems (*20*). These studies have included both a reduction of the channel diameter [0.44 to 0.55 nm for theta-1 (*9*)] and an enhancement of the molecular diameter [0.47 nm for tetrafluoromethane (CF_4) (*19*)]. In all cases, the measured mean square displacements were found to follow Eq. 2. Two typical examples are included in Fig. 2. As expected, both an increase in the molecular diameter and a reduction in the channel diameter effect a reduction of the mobility (Table 1). Taken together, these results constitute direct evidence of single-file diffusion in zeolites with a 1D channel structure.

Table 1. Results of the PFG NMR measurement of molecular diffusion in a variety of zeolites with a 1D channel structure at 293 K. The host zeolites are described in the reference listed in the first column.

Guest-host system	Mean crystal length (μm)	Concentration (molecules per unit cell)	Range of observation times (ms)	F (ms^2 s$^{-1/2}$)
CH_4-$AlPO_4$-5 (*21*)	120	0.2	0.8–400	6×10^{-11}
CH_4-$AlPO_4$-5 (*22*)	25	0.2	2–60	6×10^{-11}
CF_4-$AlPO_4$-5 (*21*)	120	0.4	4–512	1×10^{-12}
CF_4-$AlPO_4$-5 (*23*)	100	0.2	4–96	2×10^{-12}
CH_4-theta-1 (*24*)	30	0.5	1.5–60	8×10^{-12}

REFERENCES AND NOTES

1. A. Bunde, L. L. Moseley, H. E. Stanley, D. Ben-Avraham, S. Havlin, *Phys. Rev. A* **34**, 2575 (1986); K. W. Kehr and K. Binder, in *Application of the Monte Carlo Methods in Statistical Physics*, K. Binder, Ed. (Springer-Verlag, Berlin, 1984), pp. 181–223.
2. P. A. Fedders, *Phys. Rev. B* **17**, 40 (1978); J. Kärger, *Phys. Rev. A* **45**, 4173 (1992); *Phys. Rev. E* **47**, 1427 (1993).
3. A. L. Hodkin and R. D. Keynes, *J. Physiol. (London)* **128**, 61 (1955); L. Rickert, *Adv. Catal.* **21**, 281 (1970); D. G. Levitt, *Phys. Rev. A* **8**, 3050 (1973).
4. E. Neher, *Science* **256**, 498 (1992); B. Sakmann, *ibid.*, p. 503.
5. D. P. Chen and R. S. Eisenberg, *Biophys. J.* **65**, 727 (1993).
6. G.-D. Lei and W. M. H. Sachtler, *J. Catal.* **140**, 601 (1993).
7. P. T. Callaghan, *Principles of Nuclear Magnetic Resonance Microscopy* (Clarendon, Oxford, 1991).
8. J. Kärger and D. M. Ruthven, *Diffusion in Zeolites and Other Microporous Materials* (Wiley, New York, 1992).
9. W. M. Meier and D. H. Olson, *Atlas of Zeolite Structure Types* (Butterworth-Heinemann, London, 1992).
10. S. Feng and T. Bein, *Science* **265**, 1839 (1994); M. Noack, P. Kölsch, D. Venzke, P. Toussaint, J. Caro, *Micropor. Mater.* **3**, 201 (1994).
11. J. Kärger, M. Petzold, H. Pfeifer, S. Ernst, J. Weitkamp, *J. Catal.* **136**, 283 (1992).
12. J. Kärger, N.-K. Bär, W. Heink, H. Pfeifer, G. Seiffert, *Z. Naturforsch. Teil A* **50**, 186 (1995).
13. N.-K. Bär, J. Kärger, C. Krause, W. Schmitz, G. Seiffert, *J. Magn. Reson. A* **113**, 278 (1995).
14. P. T. Callaghan, *J. Magn. Reson.* **88**, 493 (1990); F. Stallmach, J. Kärger, H. Pfeifer, *J. Magn. Reson. A* **102**, 270 (1993).
15. P. T. Callaghan, *Aust. J. Phys.* **37**, 359 (1984); J. Kärger, H. Pfeifer, H., W. Heink, *Adv. Magn. Reson.* **12**, 1 (1988).
16. E. O. Stejskal and J. E. Tanner, *J. Chem. Phys.* **42**, 288 (1965).
17. F. Schüth, *J. Phys. Chem.* **96**, 7493 (1992); F. Marlow and J. Caro, *Zeolites* **12**, 433 (1992).
18. S. S. Nivarthi, A. V. McCormick, H. T. Davis, *Chem. Phys. Lett.* **229**, 297 (1994).
19. D. W. Breck, *Zeolites: Molecular Sieves* (Wiley, New York, 1974), p. 636.
20. V. Kukla, in preparation.
21. J. Kornatowski, G. Finger, J. Richter-Mendau, M. Bülow, *Zeolites* **11**, 443 (1991).
22. I. Girnus, K. Jancke, R. Vetter, J. Richter-Mendau, J. Caro, *ibid.* **15**, 33 (1995); I. Girnus *et al.*, *Adv. Mater.* **7**, 711 (1995).

23. D. Demuth, G. D. Stucky, K. K. Unger, F. Schüth, *Micropor. Mater.* **3**, 473 (1995).
24. D. M. Shen and L. V. C. Rees, *J. Chem. Soc. Faraday Trans.* **90**, 3017 (1994).
25. We are obliged to many colleagues, in particular, to K. Arnold, J. Caro, K. Hahn, K. Kehr, L. Riekert, D. M. Ruthven, and J. Weitkamp, for stimulating discussions on the phenomenon of single-file diffusion. Financial support was provided by the Deutsche Forschungsgemeinschaft (Graduiertenkolleg "Physical Chemistry of Interfaces" and Sonderforschungsbereich 294).

18 December 1995; accepted 6 March 1996

Photoinduced Magnetization of a Cobalt–Iron Cyanide

O. Sato, T. Iyoda, A. Fujishima,* K. Hashimoto*

Photoinduced magnetization was observed in a Prussian blue analog, $K_{0.2}Co_{1.4}[Fe(CN)_6]\cdot 6.9H_2O$. An increase in the critical temperature from 16 to 19 kelvin was observed as a result of red light illumination. Moreover, the magnetization in the ferrimagnetic region below 16 kelvin was substantially increased after illumination and could be restored almost to its original level by thermal treatment. These effects are thought to be caused by an internal photochemical redox reaction. Furthermore, blue light illumination could be used to partly remove the enhancement of the magnetization. Such control over magnetic properties by optical stimuli may have application in magneto-optical devices.

The design of molecule-based compounds exhibiting spontaneous magnetization with high critical temperature, T_c, is one of the main challenges in molecular materials science. Compelling results have recently been reported (*1–11*). Current research in this field aims not only to improve magnetic properties, but also to achieve unusual properties, which to date have not been realized in magnets. Our objective is the production of magnets with magnetic properties that can be controlled by external stimuli (Fig. 1). We previously reported an electrochemically tunable molecule-based magnet (*12*). Another possibility is the induction of a magnetic phase transition by optical stimuli. This subject is of considerable importance because the photon mode allows access to a variety of different types of materials with high speed and superior resolution. We now report photoinduced magnetization changes observed in a cobalt–iron cyanide.

A photoinduced memory effect can be triggered by an electronic excitation in a given material that induces the rearrangement of the lattice, resulting in the formation of a new phase after relaxation (*13*). This new phase may have modified magnetic properties. The material we chose in our experiments was a cobalt–iron cyanide–based Prussian blue analog. A compound with a stoichiometry of $Co^{II}{}_3[Fe^{III}(CN)_6]_2$ (T_c = 14 to 15 K) has already been reported (*14–17*). The reaction of $K_3Fe^{III}(CN)_6$ and $Co^{II}Cl_2$ in aqueous solution produces a dark purple precipitate (*18*). Elemental analysis yields the formula $K_{0.2}Co_{1.4}[Fe(CN)_6]\cdot 6.9H_2O$ (*19*), hereafter designated as compound 1. The powder x-ray diffraction pattern was consistent with a face-centered cubic structure (unit cell parameter = 10.28 Å) (Fig. 1). The optical absorption spectrum is shown in Fig. 2. The infrared (IR) spectrum measurement at 12 K in the region from 2000 to 2200 cm^{-1} showed three peaks: a strong peak at 2162 cm^{-1}, a weak peak at 2116 cm^{-1}, and a shoulder at 2097 cm^{-1}. The CN stretch for $Co^{II}{}_3[Fe^{III}(CN)_6]_2$ was observed at 2160 cm^{-1}, whereas that for $Co^{II}{}_2[Fe^{II}(CN)_6]$ was observed at 2085 cm^{-1} (*16*). The peak at 2116 cm^{-1} appears when K^+ is included in the compounds. Thus, we think that the peak at 2162 cm^{-1} is due to the stretching of CN in Fe^{III}-CN-Co^{II} links at positions where no K^+ ion is located in interstitial sites, and the peak at 2116 cm^{-1} can be assigned to the stretching of CN groups that surround K^+ ions. The relatively low frequency of the CN stretch (2116 cm^{-1}) indicates that the oxidation states of the metals in Fe-CN-Co moieties exhibiting this frequency can be expressed as Fe^{II}-CN-Co^{III}. The peak at 2097 cm^{-1} is probably due to the CN stretch of Fe^{II}-CN-Co^{II} moieties, but this is not clear at present. Magnetic properties were investigated with a superconducting quantum interference device (SQUID) magnetometer (Quantum Design MPMS-5S). The product of the molar magnetic susceptibility and temperature, $\chi_M T$, versus T plot first decreased upon cooling and then increased at lower temperatures, indicating a short-range antiferromagnetic interaction between paramagnetic centers bearing different numbers of unpaired electrons (ferrimagnetism). The $\chi_M{}^{-1}$ versus T plots became almost linear in the paramagnetic region below 150 K. The Curie constant, C, and the Weiss constant, θ, were 3.4 $cm^3\ mol^{-1}$ K and −8 K, respectively. The field-cooled magnetization (FCM) versus temperature plots at H = 5 G displayed an abrupt break at T_c = 16 K. The field dependence of the magnetization yielded a magnetization at 5 T of about 2.2 Bohr magnetons per $K_{0.2}Co_{1.4}[Fe(CN)_6]\cdot 6.9H_2O$ moiety.

A Hg-Xe lamp was used as the light source in the investigation of the photoinduced magnetic effects. The filtered red light (660 nm with 50-nm half-width, 3.5 mW/cm^2) was guided by optical fiber into the SQUID magnetometer for illumination of the sample. Upon irradiation at 5 K, the magnetization at 5 G increased rapidly and then gradually saturated after several tens of minutes (*20*). The enhancement effect persisted for periods of several days at 5 K. The FCM was measured as a function of temperature before and after light illumination at 5 K (Fig. 3). The T_c after the irradiation was about 19 K, which was 3 K higher than the T_c of the material before illumination. Furthermore, the magnetization was substantially enhanced in the entire temperature

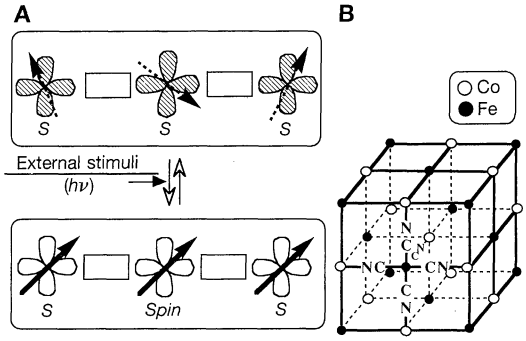

Fig. 1 (left). (**A**) Control of spins in magnetic materials. (**B**) Unit cell of compound 1. Interstitial K^+ ions, water molecules, and defects in the unit cell have been omitted for clarity. **Fig. 2 (right).** Optical absorption spectrum of compound 1.

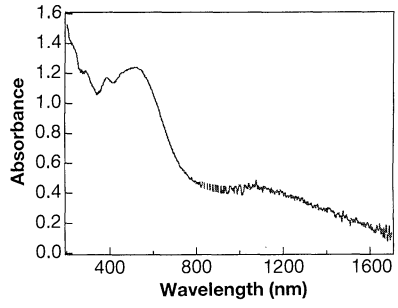

O. Sato and T. Iyoda, Kanagawa Academy of Science and Technology, Tokyo Institute of Polytechnics 1583 Iiyama Atsugi, Kanagawa 243-02, Japan.
A. Fujishima, Department of Applied Chemistry, University of Tokyo, 7-3-1 Hongo, Bunkyo-ku, Tokyo 113, Japan.
K. Hashimoto, Kanagawa Academy of Science and Technology, Tokyo Institute of Polytechnics, 1583 Iiyama, Atsugi, Kanagawa 243-02, and the Department of Applied Chemistry, University of Tokyo, 7-3-1 Hongo, Bunkyo-ku, Tokyo 113, Japan.

*To whom correspondence should be addressed.